Magnetic analysis of rapidly quenched LaFe alloys-a ferromagnetically coupled ferromagnetic cluster system: I. Experimental results

1994 J. Phys.: Condens. Matter 6 9393

(http://iopscience.iop.org/0953-8984/6/44/018)

J. Phys.: Condens. Matter 6 (1994) 9393–9404. Printed in the UK

Magnetic analysis of rapidly quenched LaFe alloys—a ferromagnetically coupled ferromagnetic cluster system: I. Experimental results

Shinichiro Kondo†¶, Eiji Kita‡, Keiichi Higashi§*, Akira Saruyama§#, Hiromitsu Ino§ and Kiiti Siratori‖

† Department of Materials Science and Engineering, Faculty of Engineering, Nagasaki University, Nagasaki, Japan

‡ Institute of Applied Physics, University of Tsukuba, Tsukuba, Ibaraki, Japan

§ Department of Materials Science, Faculty of Engineering, University of Tokyo, Bunkyo, Tokyo, Japan

‖ Department of Physics, Faculty of Science, Osaka University, Toyonaka, Osaka, Japan

Received 22 February 1994, in final form 28 June 1994

Abstract. LaFe alloys of 1–25 at.% Fe were rapidly quenched from the melt and investigated magnetically. α-Fe was not detected in the alloys with less than 12% Fe. It was concluded that the alloys are composed of small ferromagnetic clusters dispersed in a non-magnetic matrix of β-La and coupled with each other to form a ferromagnet as a whole below about 250 K. Ferromagnetism in a cluster disappeared at around 400 K, suggesting the formation of a metastable intermetallic compound unknown so far. The existence of non-magnetic Fe atoms dissolved in β-La was detected in the 1% Fe alloy. Annealing at 400 °C for 30 min changed the cluster to antiferromagnetic at room temperature, indicating the existence of another intermetallic compound. Except for the absolute magnitude of the magnetization, the magnetic properties of the alloys did not depend on the Fe concentration. The quenching process of the alloys is discussed based on this fact.

1. Introduction

Rare earth–transition metal systems have been the target of investigations in physics and metallurgy. In recent years, the discovery of useful materials such as the Nd–Fe–B permanent magnet has added special interest to the systems. La–Fe is one example of a ferromagnetic transition metal in combination with a rare earth with vacant 4f levels. In thermal equilibrium, however, no intermetallic compound is believed to exist and the solubility limit is effectively zero on both sides. Part of the equilibrium phase diagram is shown in figure 1. The eutectic point is at about 8.5 at.% Fe, 780 °C. The report of the formation of $LaFe_5$ and $LaFe_2$ as stable compounds is rather doubtful [1].

In the La–Fe system, formation of the amorphous phase was reported by sputtering on a cooled substrate in the concentration range of about 10–90 at.% Fe. Within this range, products are single-phase between 65 and 83% Fe [2]. On the other hand, rapid quenching

¶ Previously at Department of Materials Science, Faculty of Engineering, University of Tokyo, Bunkyo, Tokyo, Japan.

* Present address: Mizushima Steelworks, Kawasaki Steel Corporation, Kurashiki, Okayama, Japan.

\# Present address: Keiyo Transport Section, East Japan Railway Company, Tokyo, Japan.

0953-8984/94/449393+12$19.50

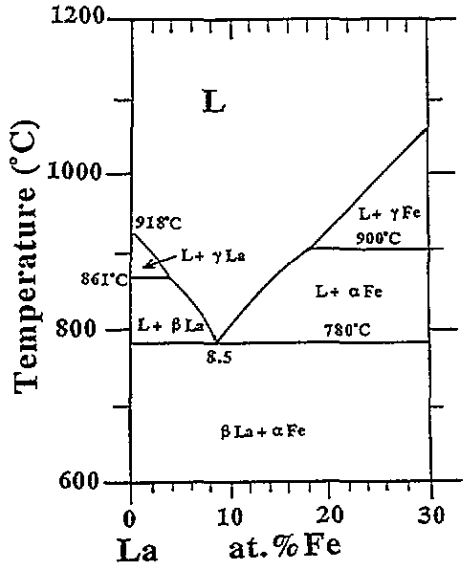

Figure 1. La–Fe phase diagram in equilibrium, the part near La.

of the melt has not yielded amorphous alloys [3–6]. Even in the crystalline state, however, there is a possibility that rapid quenching results in states different from those in equilibrium. The solubility limit can be finite and metastable intermetallic compounds can appear.

Here, we will report the production of metastable intermetallic compounds as clusters in the La matrix as well as the existence of non-magnetic Fe atoms dissolved in β-La, which form when the melt is rapidly quenched. In the as-quenched state, the intermetallic compounds are dispersed as small ferromagnetic clusters in the non-magnetic β-La and show super-paramagnetic character below about 400 K. Below about 250 K, inter-cluster coupling makes the whole system ferromagnetic. Another antiferromagnetic compound appears by annealing at 400 °C. Since pure β-La metal is Pauli paramagnetic, magnetic analysis is effective for La-based alloys.

In the next section, experimental procedures and results are described. The results are discussed and several conclusions are drawn in section 3. Analyses of the results based on the scaling of thermal energy by $T - T_c$, where T_c is the Curie temperature due to the inter-cluster magnetic interaction, or on the molecular-field approximation are presented in the subsequent paper [7], which will be referred to as II hereafter.

Preliminary reports of this investigation were made at the international conference 'Rare Earths '92', Kyoto, 1992, and have been published elsewhere [4–6, 8].

2. Experimental methods and results

The starting materials, La metal containing 1, 4, 8, 12, 20 and 25 at.% Fe, were prepared by arc-melting a mixture of the two metals in an argon atmosphere. Specimens of about 2 g were cut from the ingot and quenched from the melt by a single-roller apparatus, in a 1 Torr helium atmosphere. Ribbons about 20–35 μm thick and 1 mm in width were obtained.

Both sides of the ribbons were examined by x-ray diffraction. Diffraction peaks of β-La, with traces of α-La, were detected for all specimens. No signs of an amorphous solid or any unknown compounds were noticed. For the samples with 20 and 25 at.% Fe,

peaks of α-Fe were observed. Specimens with segregated Fe are beyond the scope of the present report, since magnetic analysis is difficult for such alloys. In the specimens with Fe concentrations lower than 12%, no Fe peaks were detected. The lattice constant of the FCC β-La, the main component, does not depend on the composition of the alloys within the accuracy of the measurements. Figure 2 shows examples of the diffraction profiles. The lattice constants of β-La are plotted in figure 3 as a function of Fe concentration, for both the as-quenched and heat-treated specimens. The fact that the lattice constant of the β-La phase is independent of Fe concentration suggests that most of the Fe atoms do not dissolve in β-La either substitutionally or interstitially.

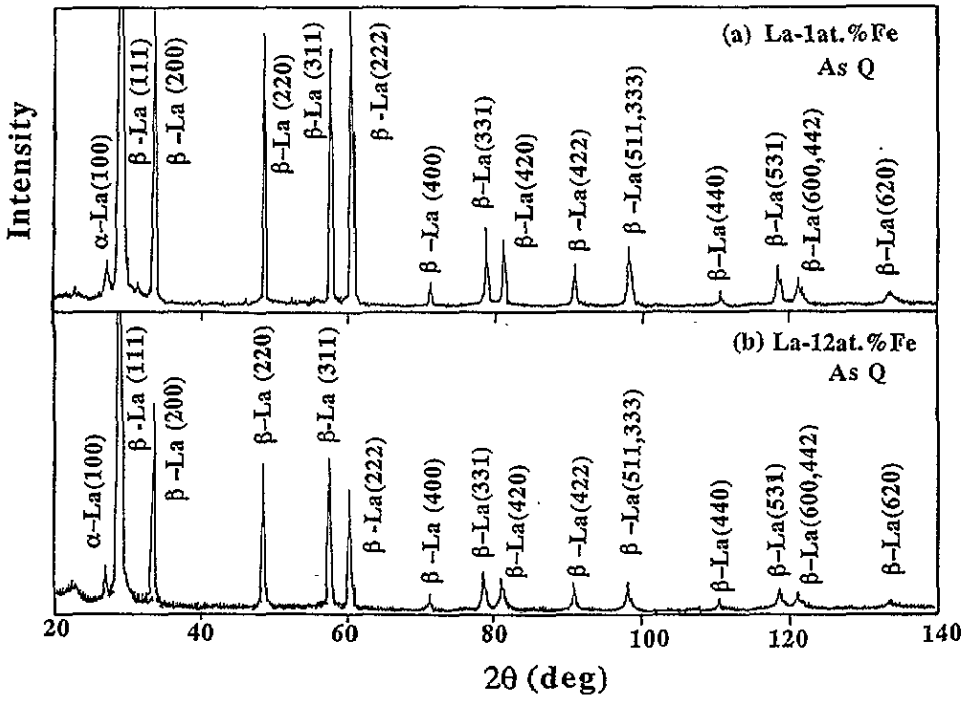

Figure 2. X-ray diffraction patterns of rapidly quenched La–1 at.% Fe (*a*) and La–12 at.% Fe (*b*) ribbons, in the as-quenched state.

A chemical analysis was performed by radiofrequency inductively coupled plasma photoemission spectroscopy for one specimen of 1% Fe (specimen 1-1), because the saturation moment at 4.2 K was much smaller than the value estimated from the nominal concentration as well as that of another 1% alloy (specimen 1-2). The result was between 0.8 and 1.2 at.% Fe, confirming the small deviation from the nominal composition.

The Mössbauer ^{57}Fe spectra were measured at room temperature and 77 K in order to determine the local configuration around Fe atoms as well as the magnetic ordering. Measurements were carried out by a conventional spectrometer, in a constant-acceleration mode. Iron enriched with ^{57}Fe was used in the 1% Fe specimen (specimen 1-2). Examples of the spectra are shown in figures 4 and 5.

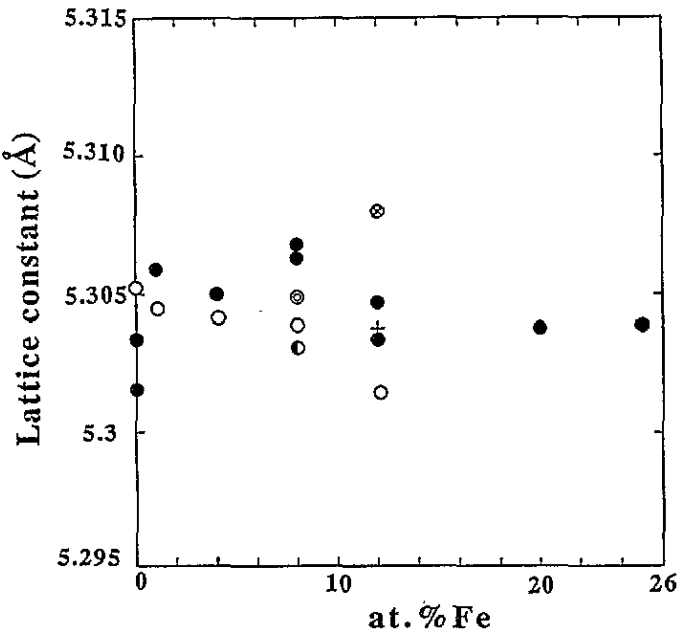

Figure 3. The lattice constants of the FCC β-La, both as-quenched and heat-treated at 400 °C, as a function of Fe concentration: (●) as quenched; (◐) annealed at 593 K for 30 min; (◎) 623 K, 30 min; (○) 673 K, 30 min; (+) 723 K, 30 min; (⊗) 953 K, 30 min.

The spectra of the as-quenched specimens showed essentially the same profile as shown in figure 4(*a*). The statistics of the spectra for 8 and 12% Fe alloys were not good, as is seen in the figure, because of the strong absorption of the 14.4 keV γ-ray by La atoms. At room temperature, the spectra revealed well defined asymmetric quadrupole doublets with an average splitting of 0.44 mm s^{-1}. This indicates that the Fe sites do not have cubic symmetry in the material, in contrast to those in α- or γ-Fe, or probable interstitial or substitutional sites in FCC β-La. The average isomer shift was -0.09 mm s^{-1} relative to α-Fe. At 77 K, a broad sextet with an average hyperfine field of about 290 kOe, together with a small amount of paramagnetic component, was observed for the as-quenched specimen (figure 4(*b*)). The distributed hyperfine field suggests lack of atomic translational symmetry or the distributed magnetic environment of Fe atoms. If we assume that the hyperfine magnetic field at the nuclei is proportional to the moment of the Fe atom, this magnitude of the hyperfine field corresponds to about $1.9\mu_B$/Fe atom.

After the specimens were heat-treated at about 400 °C (= 673 K) for 30 min, the spectra of 8 and 12% specimens at 300 K changed into a broad sextet with an average hyperfine field of 240 kOe, together with a subspectrum from the component of α-Fe. In the case of the 1% Fe specimen, the main component was a paramagnetic doublet with an isomer shift of -0.19 mm s^{-1} and a quadrupole splitting of 0.61 mm s^{-1} (see figure 5).

Magnetic measurements were carried out between 4.2 and 1100 K mainly by vibrating sample magnetometers, one for the measurement from 4.2 to 600 K and another for 77 to 1100 K, and supplemented by a SQUID (superconducting quantum interference device) magnetometer at low temperatures. In the measurements with the SQUID, an external

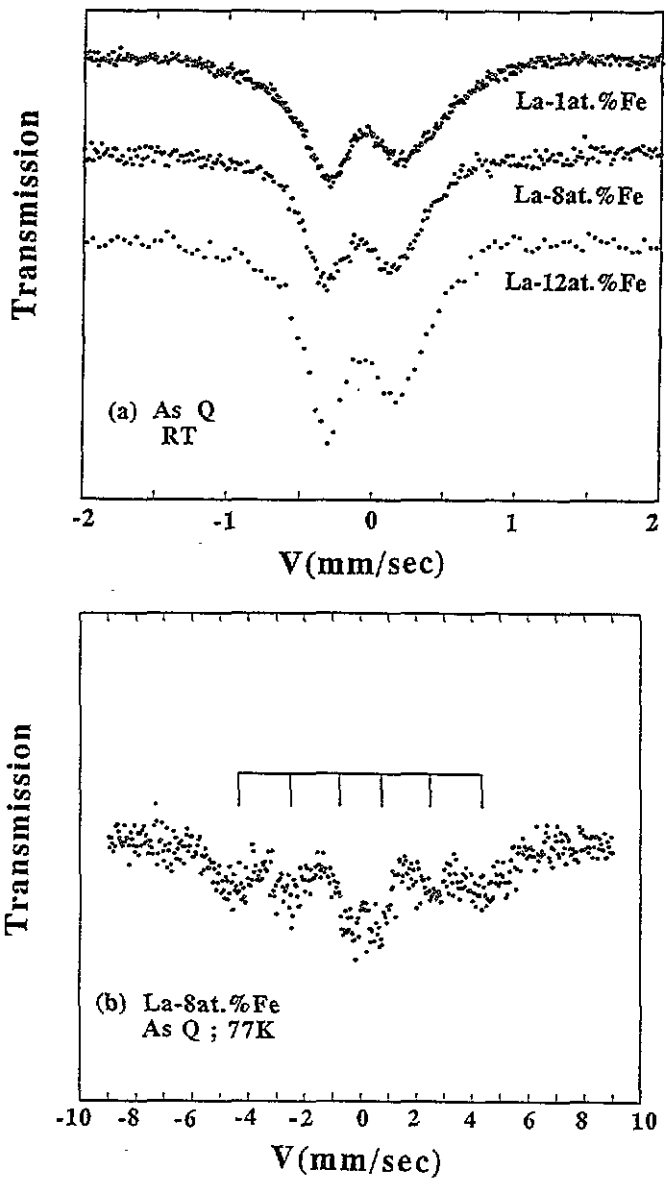

Figure 4. Mössbauer spectra of LaFe rapidly quenched alloys. (*a*) As-quenched (state A) specimen of 1, 8 and 12% alloy, at room temperature. (*b*) As-quenched (state A) 8% alloy, at 77 K.

magnetic field up to 50 kOe was applied.

Examples of magnetization curves, measured at 300, 77 and 4.2 K for the as-quenched 8% Fe specimen, are shown in figure 6. All curves are non-linear and tend towards saturation at high applied field. The non-linear magnetization curve without hysteresis and the absence of the hyperfine field in the Mössbauer spectrum, observed at room temperature, are typical characteristics of super-paramagnetism. On the other hand, hysteresis observed at low temperatures suggests ferromagnetism below room temperature.

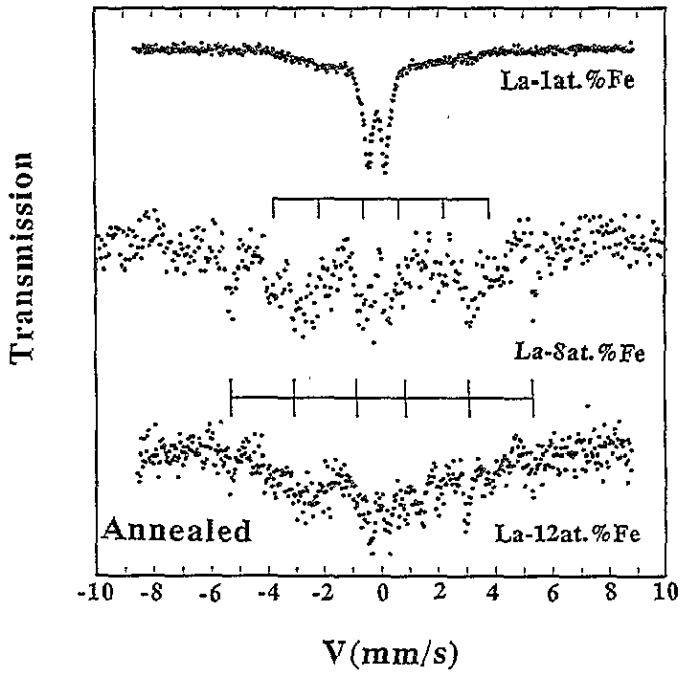

Figure 5. Mössbauer spectra of LaFe rapidly quenched alloys at room temperature. Specimens of 1, 8 and 12 at.%, annealed at 400 °C for 30 min (state B). Vertical lines between the lower two spectra indicate absorption lines of α-Fe.

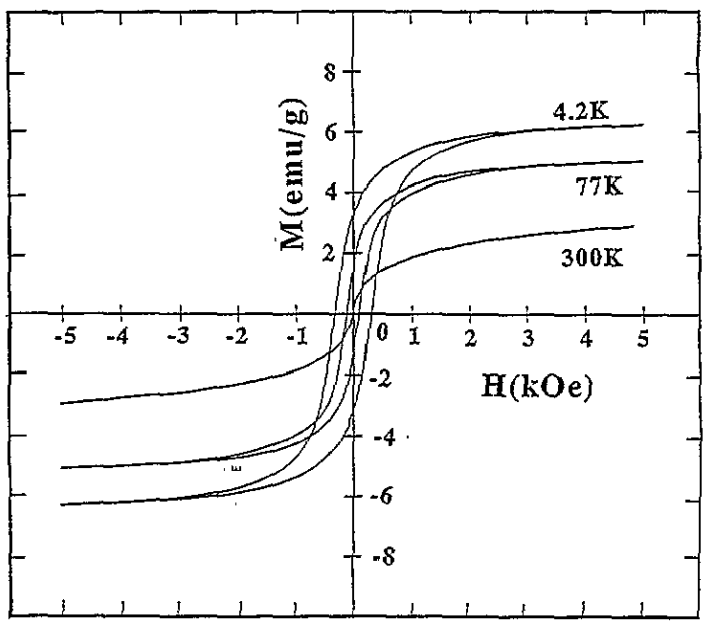

Figure 6. Magnetic hysteresis curves of the as-quenched 8% Fe alloy at 300, 77 and 4.2 K.

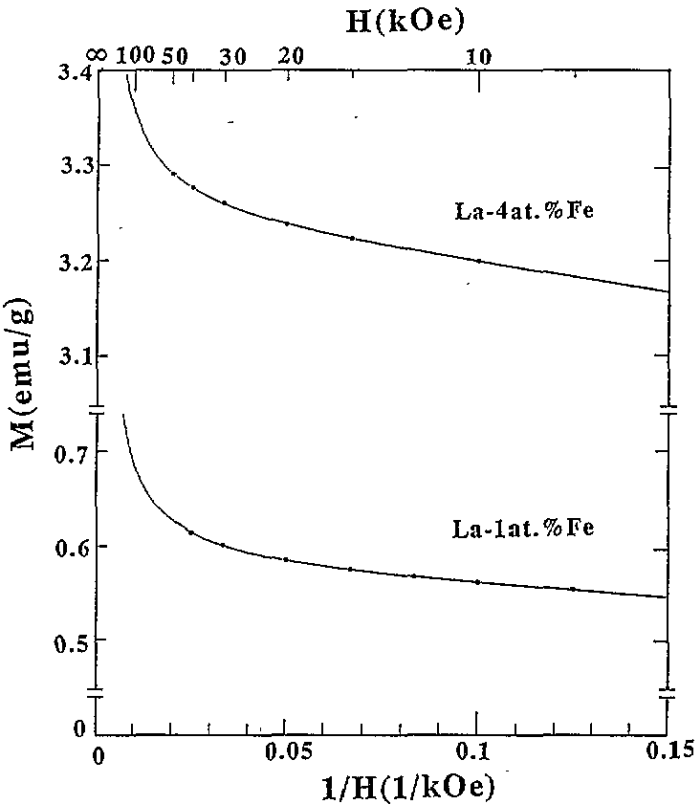

Figure 7. The approach to saturation magnetization at 5 K, for 1(−2) and 4% Fe as-quenched alloys. Curves are due to equation (1).

Figure 7 shows examples of magnetization curves at 5 K. Measured magnetizations are expressed very well by the following equation

$$M = M_0 - C/H + \chi_p H \tag{1}$$

as shown by the smooth curves in the figure. No other term, proportional to $1/H^{1/2}$, etc, is necessary. The parameters M_0, C and χ_p are tabulated in table 1. Apparently, the third term is Pauli paramagnetism of La. As is shown below, this system is a set of ferromagnetic clusters dispersed in the paramagnetic La matrix. Then, the first term is the saturation magnetization of the cluster system. The second term is tentatively interpreted as the tail of the Langevin function.

Since the saturation magnetization estimated from the curve is only one-third of the calculated value for the sample 1-1, whereas chemical analysis of the sample gave 1.0 ± 0.2 at.% for the Fe concentration, we can conclude that non-magnetic Fe atoms exist in the alloy. As for the sample 1-2, the estimated saturation magnetization was still smaller than the calculated value but more than twice that of the sample 1-1. The saturation moments of more than 4 at.% Fe alloys do not depend so much on the specimens, though not shown in the table. Apparently, the amount of non-magnetic Fe decreases with increasing Fe concentration.

Table 1. Parameters for the magnetization curves at 5 K[a].

Specimen	Full moment[b] (emu g^{-1})	M_0 (emu g^{-1})	C (emu MOe g^{-1})	χ_p (10^{-6} emu g^{-1})
1-1	0.808	0.229	1.67	1.4
1-2	0.808	0.574	2.41	1.2
4	3.29	3.24	5.51	1.2
8	6.75	6.72	14.93	1.2
12	10.04	10.61	17.16	0.4

[a] Magnetization curves are expressed as $M = M_0 - C/H + \chi_p H$ (see figure 7).
[b] Calculated value by the nominal concentration of Fe and an assumption of 2.0μ_B/Fe.

Both samples with 1% Fe disclosed superconductivity at 5 K. For the specimens with higher Fe concentration, the Meissner effect was not observed at this temperature. We have not extended our measurements below 4.2 K.

Figure 8 gives examples of the temperature dependence of magnetization during heating, above room temperature in an external field of 5 kOe. Four different states of the specimen are demonstrated, as designated in the figure: (A) as-quenched, up to about 600 K; (B) at 650–900 K; (C) at 950–1000 K; and (D) above 1000 K. The most interesting point is that the features of the curves are not dependent on Fe concentration, except the scale of the ordinate. Multiplication of each magnetization by proper factors will result in almost the same thermomagnetic curves, irrespective of Fe concentration.

There is no doubt that D indicates precipitation of α-Fe, appearing just below the eutectic temperature of the alloy (see figure 1). This argument is supported by the magnetization measurements at 996 K, which showed the existence of a spontaneous moment. Little is known about state C. As is shown, this part is sample-dependent. The present experiments were carried out mainly on the states A and B.

According to figure 9, showing the thermomagnetic curves of A and B at low temperatures in an external field of 100 Oe, a magnetic transition is implied in state A at around 300 K. Magnetic hysteresis curves (figure 6) and Mössbauer spectra (figure 4) at temperatures below 300 K strongly suggest that this is a transition from super-paramagnetic to ferromagnetic state. Figure 8 suggests that the super-paramagnetism, or the ferromagnetism within clusters, disappears at around 400 K.

The change from state A to B is irreversible: not magnetic but structural. The magnitude of the magnetization of the state B above 600 K, increased over that of state A (see figure 8), keeps its value when cooled down to room temperature (see figure 9). A slight increase of the magnetization in B at 300 K, the temperature where the magnetization of A increases, suggests that the transformation from A to B has not been completed by an annealing of 30 min at 670 K.

The magnetization curve of the state B is not linear with the external field but saturates even at 670 K. It is to be noted that the precipitation of α-Fe was detected by the Mössbauer spectrum of the state B (figure 5) at room temperature, except for the specimen of 1% Fe. It is very likely that the ferromagnetic moment detected in state B can be explained totally by the precipitation of a small amount of α-Fe and the remnant of the state A. At the same time, the Mössbauer spectrum at room temperature indicates the ordering of all Fe spins in alloys of higher Fe concentration: state B is antiferromagnetic. The ordering temperature has not been determined.

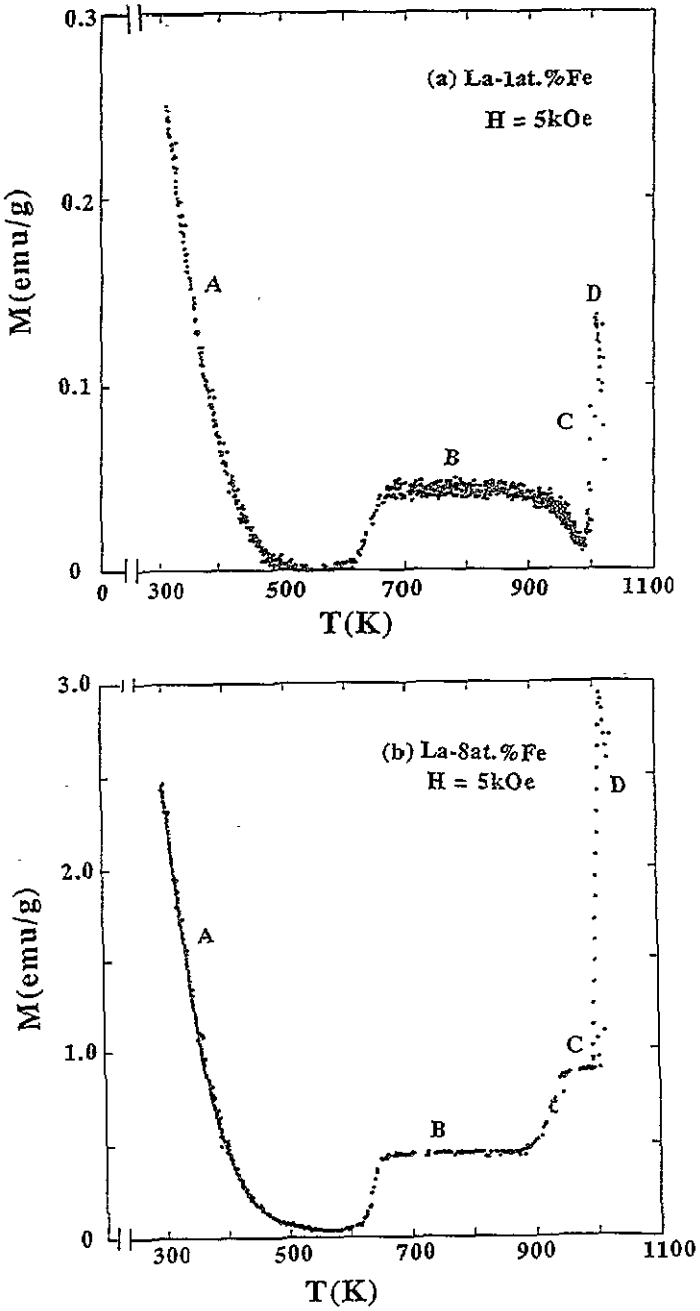

Figure 8. Thermomagnetic curves of LaFe rapidly quenched alloys, indicating four different states A to D. An external field of 5 kOe was applied. (*a*) 1 at.% Fe (specimen 1-2) and (*b*) 8 at.% Fe.

3. Discussion

3.1. Metastable intermetallic compounds between La and Fe

Thermomagnetic curves in figures 8 and 9 indicate two magnetic transitions in as-quenched

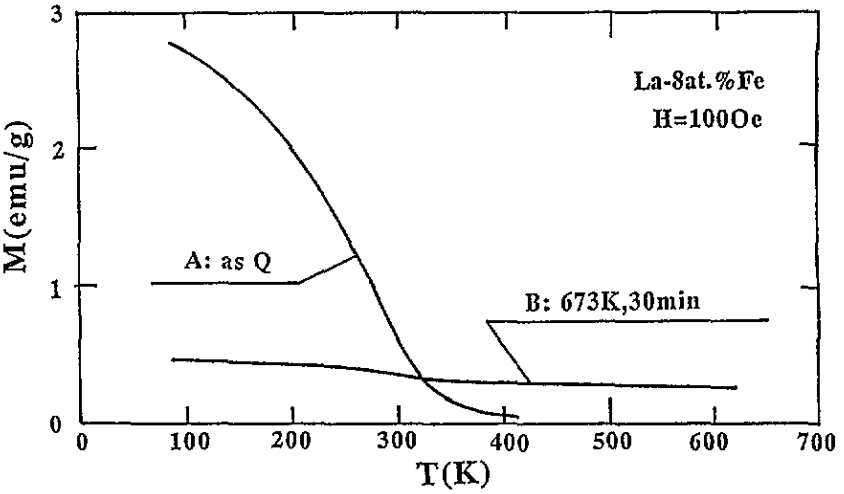

Figure 9. Thermomagnetic curves of state A (as-quenched) and state B (heat-treated at 400 °C for 30 min) of 8% Fe alloy. The external field was 100 Oe.

alloys of this system: from paramagnetic to super-paramagnetic at around 400 K and from super-paramagnetic to ferromagnetic at around 300 K. Though the appearance of super-paramagnetism at room temperature is confirmed, determination of the transition points is not easy on both high- and low-temperature sides. The usual $1/\chi$ versus T plot does not result in a straight line in a wide temperature range, as shown in figure 10. This is due to the transition from A to B during the measurements at temperatures higher than 500 K and to the saturation of magnetization because of the large moment of clusters at temperatures near 300 K. We can confirm only the two-step decrease of magnetization in figure 10. Scaling of magnetization and thermal energy, however, make estimations possible for the magnitude of asymptotic Curie temperatures, for both the inter- and intra-cluster coupling, as well as the average size of clusters. Details of the analysis are described in II.

The Curie temperatures of a cluster, T_C^{intra} in table 1 of II, are about 430 K, almost the same for the five specimens (see figure 8). This is much lower than 1050 K, the Curie temperature of α-Fe, indicating that the magnetic clusters are not α-Fe but an unknown intermetallic compound between La and Fe (refer to our explanation of the state D in figure 8 by the precipitation of α-Fe). A Curie temperature of 430 K is not unexpected for an intermetallic compound of a rare earth and iron. The small size of clusters, 100–1000 Fe atoms, will explain the wide distribution of hyperfine magnetic field at ^{57}Fe nuclei and the absence of x-ray diffraction peaks. On the other hand, superstructure in an FCC lattice was detected by electron diffraction over a limited portion of the specimen [8, 9]. Determination of the structure is a task for the future.

The Mössbauer and magnetic measurements at 300 K of the specimens annealed at 400 °C for 30 min (state B) indicate antiferromagnetism as was discussed in the last section (see figures 5 and 9). This means that there exists another metastable intermetallic compound in the La–Fe system. Observation of the finite internal field at 300 K, in contrast to the state A, suggests increase of the cluster size during annealing. Small-angle neutron scattering experiments support this argument [10].

3.2. Process of the formation of clusters

One of the interesting results of the present experiment is that the magnetic properties of the

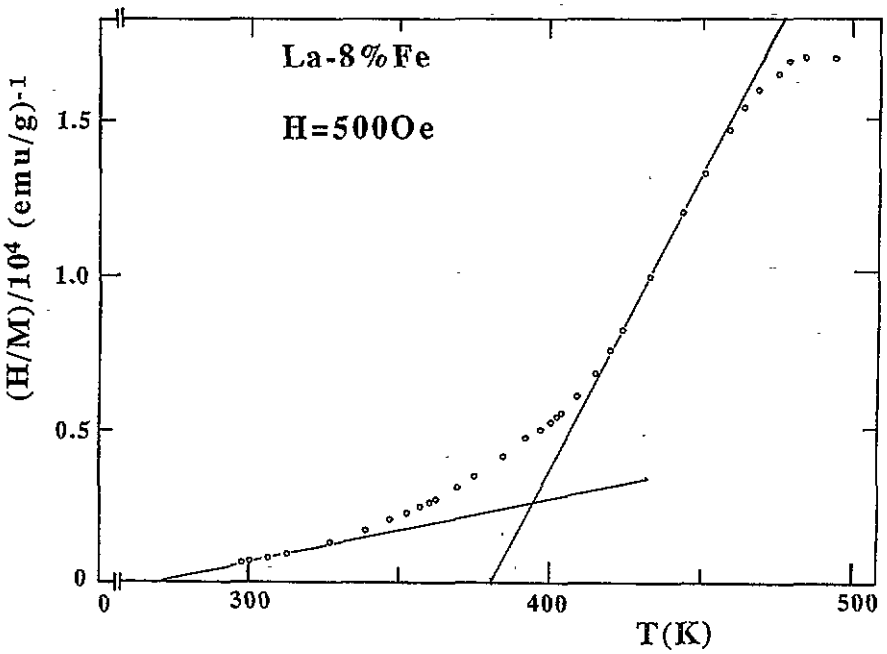

Figure 10. Plot of H/M of the 8% Fe as-quenched alloy in an external field of 500 Oe, above 300 K.

system do not depend on the Fe concentration except for the magnitude of the magnetization. This fact strongly suggests that the precipitation of magnetic clusters occurs in a similar situation irrespective of Fe concentration, from 1 to 12%. That is easily understood if the clusters are formed via the following two-step process.

Step 1: an iron-poor La phase segregates from the starting homogeneous liquid, resulting in the formation of an iron-rich liquid phase.

Step 2: clusters are formed in this iron-rich matrix during subsequent cooling.

It is natural to assume that the first step takes place along the liquidus line, perhaps with a little modification, of the equilibrium phase diagram (figure 1). Then, the concentration of Fe in the iron-rich matrix will be determined as a function of temperature, independent from the starting composition. If the magnetic clusters start to segregate at a certain temperature, presumably with solidification of the liquid, the density of clusters in the matrix will be nearly the same.

Such a process of segregation of clusters means that they will not distribute homogeneously in the β-La matrix but concentrate around certain regions where Fe-poor La phase segregates in the first stage. Annealing of the alloys can eliminate this secondary structure. This was observed in small-angle neutron and x-ray scattering experiments [10].

According to the present experiments, precipitation of α-Fe is suppressed, at least up to 12 at.% Fe, by supercooling of the liquid along the extrapolated liquidus line. At the end of the first stage, the composition of Fe in the concentrated alloy might be $\geqslant 12\%$ and thus the Fe composition of the magnetic clusters should be higher than 12%. If we tentatively assume that magnetic clusters with the same volume are formed regularly and their composition is $LaFe_2$, cluster–cluster distance (surface to surface) is about 0.8 times the cluster diameter. The diameter of a cluster of 150 Fe atoms will be about 17 Å (see II).

3.3. Existence of non-magnetic Fe atoms in β-La

In the first stage of the quenching process, the segregation of the Fe-poor La phase from the melt, a small number of Fe atoms can dissolve in La.

The 3d electrons of an Fe atom isolated in a metal will not localize to form a magnetic moment but will be itinerant, leaving the Fe atoms non-magnetic, when the density of states of the conduction band of the matrix is large at the 3d level of Fe. We can assume such a situation for the 1% alloy of the present case.

In the case of the higher concentration alloys, in contrast to the 1% alloy, the saturation moment coincides with the magnitude expected from the nominal composition, within the experimental accuracy. This can be explained by the fact that the segregation of the La phase along the liquidus line starts at higher temperatures in the alloys with lower Fe concentration. At higher temperatures, the non-equilibrium La phase is expected to contain more solute atoms.

It is interesting to note that the phase boundary between the FCC β-La and the BCC γ-La, at about 860 °C, crosses the liquidus line at about 3.5 at.% Fe. In the case of the 1% Fe alloy, γ-La segregates first and then transforms to β. There is a possibility that the BCC γ-La can dissolve more Fe atoms than the FCC β-La and the dissolved Fe atoms remain in the La matrix after the transformation of La from γ to β. If this is the case, more Fe atoms will dissolve in La in the 1% alloy than 4% or higher concentration alloys. The amount of dissolved Fe is expected to become sensitive to the quenching conditions. More experiments are necessary on this point.

Acknowledgments

The authors would like to express their thanks to Professor M Tanaka of Tohoku University for showing them the electron diffraction data prior to publication. Critical reading of the manuscript is acknowledged with hearty thanks to Professor Y Nakagawa of Tokoku University and Professor M B Salamon and Dr K Pettit of the University of Illinois, for both physics and English. Numerical calculation was carried out at the Computation Center of Osaka University.

References

[1] Kubaschewski O 1982 *Iron—Binary Phase Diagrams* (Berlin: Springer)
[2] Takemura K, Kataoka N, Sumiyama K and Nakamura Y 1989 *J. Japan. Inst. Met.* **53** 8 (in Japanese)
[3] Kawano K, Ino H and Nishikawa S 1978 *Scr. Metall.* **12** 333
[4] Kondo S, Kita E, Siratori K, Tokumitsu K and Ino H 1988 *Proc. 5th JIM Int. Symp. on Non-Equilibrium Solid Phases of Metals and Alloys (Japanese Institute of Metals); Suppl. Trans. JIM* **29** 379
[5] Kondo S, Kita E, Siratori K and Ino H 1990 *J. Japan. Inst. Met.* **54** 125 (in Japanese)
[6] Kondo S, Kita E, Siratori K and Ino H 1991 *Mater. Sci. Eng.* A **133** 226
[7] Siratori K, Kita E, Kondo S and Ino H 1995 *J. Phys.: Condens. Matter* **7** 9405
[8] Siratori K, Kita E, Kondo S, Tanaka M and Ino H 1993 *J. Alloys Compd.* **193** 249
[9] Tanaka M unpublished
[10] Kita E, Kondo S, Ino H, Furusaka M, Siratori K, Lee H and Chen H 1994 in preparation